



Log-periodic oscillations and noise-free stochastic multiresonance due to self-similarity of fractals

A. Krawiecki ^{a,*}, K. Kacperski ^b, S. Matyjaśkiewicz ^{a,c}, J.A. Hołyst ^{a,d}

^a Faculty of Physics, Institute of Physics, Warsaw University of Technology, ul. Koszykowa 75, PL-00-662 Warsaw, Poland

^b Department of Physics, Queen Mary College, University of London, Mile End Road, London E1 4NS, UK

^c Institute of Physics, Humboldt University at Berlin, Invalidenstraße 110, D-10115 Berlin, Germany

^d Max Planck Institute for the Physics of Complex Systems, Nöthnitzerstraße 38, D-01187 Dresden, Germany

Communicated by T. Kapitaniak

Abstract

The origin of log-periodic oscillations around the power-law trend of the escape probability from a precritical attractor and of the noise-free stochastic multiresonance, found in numerical simulations in chaotic systems close to crises is discussed. It is shown that multiple maxima of the spectral power amplification vs. the control parameter result from a fractal structure of a precritical attractor colliding with a possibly fractal basin of attraction at the crisis point. Qualitative explanation of the multiresonance, based on a concept of fractal self-similarity, or discrete-scale invariance, is given and compared with numerical results and analytic theory using a simple geometric models of the colliding fractal sets.

© 2003 Elsevier Science Ltd. All rights reserved.

1. Introduction

Stochastic resonance (SR) is a phenomenon occurring in systems driven by a combination of a periodic signal and random noise, such that the periodic component of a suitably defined output signal becomes most pronounced for non-zero input noise intensity [1–5]. A related phenomenon is noise-free (or deterministic) SR which appears in periodically driven chaotic systems without external random forcing, in which the internal chaotic dynamics can be tuned, by varying the control parameter, to achieve the maximization of the periodic component of the output signal [6–12]. An extension of SR is a phenomenon called stochastic multiresonance (SMR) in which the periodic component of the output signal is maximized for many values of the input noise intensity [13–15]. In the case of models that can be reduced to a particle moving in a potential field, driven by noise and a weak periodic force, SMR can appear as a consequence of a particular form of the potential [13,14]. For example, when it is invariant with respect to a discrete scaling transformation, the strength of the periodic component of the output signal shows log-periodicity as a function of the input noise intensity. A similar phenomenon, noise-free SMR [10,11], has been recently observed in chaotic maps close to crises [16,17], in which the control parameter had a small component periodic in time. This effect was explained as resulting from the collision of the fractal precritical attractor and, possibly also fractal, basin of attraction at the crisis point. It was shown that collision of these fractal sets is responsible for the appearance of oscillations around the power-law trend of the escape probability from the precritical attractor as a function of the control parameter [16,18,19]. As a result, the periodic component of the output signal, defined so that it reflected the escape events of the

* Corresponding author. Tel.: +48-22-660-79-58; fax: +48-22-628-21-71.

E-mail addresses: akraw@if.pw.edu.pl (A. Krawiecki), k.kacperski@qmul.ac.uk (K. Kacperski), matyjas@if.pw.edu.pl, matyjas@physik.hu-berlin.de (S. Matyjaśkiewicz), jholyst@if.pw.edu.pl, jholyst@mpipks-dresden.mpg.de (J.A. Hołyst).

phase trajectory from the precritical attractor, showed multiple maxima as a function of the mean value of the control parameter. However, possible relationship between the above-mentioned models for SMR in stochastic and chaotic systems has not been yet studied in more detail.

In this paper we present numerical evidence for the oscillations of the escape probability and for the noise-free SMR in chaotic maps close to crisis. Then we propose approximate description of these phenomena in terms of fractal self-similarity, which is just another name for discrete-scale invariance, or invariance with respect to a discrete scaling transformation [20]. Such a description resembles that for stochastic models of SMR studied in Refs. [13,14]. In particular, it is predicted that both oscillations of the escape probability and the strength of the periodic component of the output signal should have a log-periodic component as functions of the control parameter, which is in agreement with numerical experiments. This shows that our models belong to a wide class of systems exhibiting various forms of log-periodicity due to discrete-scale invariance, which range from, e.g., diffusion in random quenched systems [21], to earthquakes [22] to stock markets close to financial crashes [23,24]. However, the fractal structures of the colliding sets are usually too complex to be described by one discrete scaling transformation, thus the theoretical predictions based on the concept of discrete-scale invariance are only qualitatively correct. These predictions are compared to the ones based on a more accurate analytic theory.

2. Systems under study and numerical results

In systems with crises below the critical value q_c of a control parameter q there exists a chaotic attractor, above it the attractor turns into a chaotic saddle as a consequence of a collision with the border of its basin of attraction. Beyond the crisis point the attractor leaks out of its basin, and consequently one observes chaotic transients, after which the phase trajectory escapes to some distant part of the phase space. We call the complement of the precritical basin of attraction a basin of escape since the escape events occur shortly after the phase trajectory enters it. The escape probability, i.e., the inverse of the average transient duration, obeys the power scaling law

$$p(q) = C(q - q_c)^\gamma, \quad (1)$$

where C is a proportionality constant and $\gamma \geq 1/2$ is the scaling exponent (henceforth, without loss of generality, we assume $q_c = 0$). However, the chaotic saddles and, possibly, basins of escape have a discrete fractal structure which cannot be entirely neglected. This discreteness is reflected in the oscillations superimposed on the basic dependence (1) [16,18,19]. One can distinguish between normal and anomalous oscillations. The normal oscillations are connected with the subsequent branches of the fractal saddle entering, with the rise of q , the basin of escape which results in the roughly log-periodic modulation of the slope of the curve $p(q)$. The anomalous oscillations, including sections in which $p(q)$ decreases against the general trend, appear if the basin of escape has also a distinct fractal structure. In general, the shape of the curve $p(q)$ is quite complex, resulting from the overlap of two incommensurate fractal structures; nevertheless, the basic log-periodic oscillations can often be distinguished.

Henceforth our attention is constrained to systems with discrete time. In order to study SR a small periodic component is added to the control parameter, $q \rightarrow q(n) = q_0 + q_1 \cos(\omega_0 n)$. The systems are then treated as threshold-crossing (TC) systems exhibiting SR [25,26], and the escape events of the phase trajectory from the precritical attractor are identified with threshold-crossing events. The output signal is defined as equal to one if at a given time step the escape event took place and zero otherwise. As a measure of the periodicity of the output signal the spectral power amplification (SPA) is used, defined as $\sigma = S(\omega_0)/q_1^2$, where $S(\omega_0)$ is the height of the peak in the output power spectral density at the periodic signal frequency. The SPA turns out to possess multiple maxima as a function of the mean value of the control parameter.

The first system under study is the Hénon map: $x_{n+1} = p - x_n^2 - Jy_n$, $y_{n+1} = x_n$ with $J = -0.3$ which shows a boundary crisis at $p_c = 1.42692111 \dots$: for $p < p_c$ a strange attractor exists, for $p > p_c$ the system diverges to infinity. In order to investigate SR $p(n) = p_0 + p_1 \cos(\omega_0 n)$ is assumed, and the TC events are defined as the departure of the phase trajectory towards infinity (after every such event the trajectory is reinjected at random on the precritical attractor and the evolution is continued after a short transient without changing the phase of the periodic signal). The following identification of parameters can be made: $q \equiv p - p_c$, $q_0 \equiv p_0 - p_c$, $q_1 \equiv p_1$.

The second system under study is the kicked spin map [27,28]. The model describes the motion of a classical magnetic moment (spin) \mathbf{S} , $|\mathbf{S}| = S$, in the field of uniaxial anisotropy and impulse transversal magnetic field $\tilde{\mathbf{B}}(t) = B \sum_{n=1}^{\infty} \delta(t - n\tau)$ given by the Hamiltonian $H = -A(S_z)^2 - \tilde{\mathbf{B}}(t)S_x$, where $A > 0$ is the anisotropy constant. The time evolution is determined by the Landau–Lifschitz equation with damping, $\dot{\mathbf{S}} = \mathbf{S} \times \mathbf{B}_{\text{eff}} - (\lambda/S)\mathbf{S} \times (\mathbf{S} \times \mathbf{B}_{\text{eff}})$, where $\mathbf{B}_{\text{eff}} = -dH/d\mathbf{S}$ and $\lambda > 0$ is the damping parameter. The equation can be integrated and denoting by \mathbf{S}_n the spin

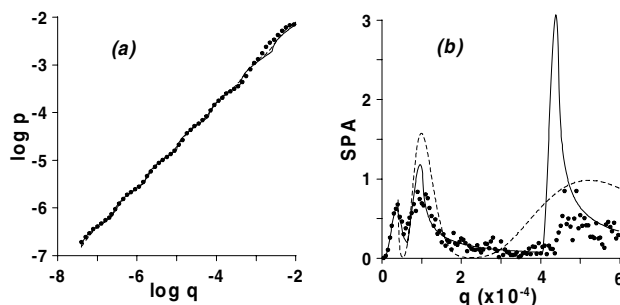


Fig. 1. Crisis in the Hénon map: (a) Mean escape probability p vs. $q \equiv p - p_c$, (b) SPA vs. $q_0 + q_1$, $q_1 \equiv p_1$; dots—numerical results, solid line—theoretical fits using the full formulae, Eqs. (4) and (7), dashed line—theoretical fits using the approximate formulae, Eqs. (11) and (12); the parameters are $p_1 = 2 \times 10^{-5}$, $T_0 = 1024$, $\alpha = 0.158$, $\eta = 0.517$, $\zeta = 0.554$, $a = 0.65$, $\gamma = 0.858$, $C = 0.467$, $B = 0.0931$, $\phi = -0.794$.

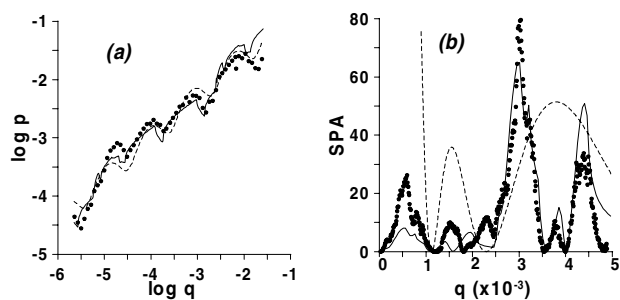


Fig. 2. As in Fig. 1, but for the crisis in the kicked spin map: the parameters are $B_1 = 3 \times 10^{-4}$, $T_0 = 1024$, $\alpha = 0.00234$, $\eta = 0.285$, $\beta = 0.124$, $b_E = 3.27$, $\zeta = 1.90$, $a = 1.05$, $b = 4.022$, $\gamma = 0.707$, $C = 0.746$, $B = -0.428$, $\phi = -0.281$.

vector just after the n th field pulse one finds a two-dimensional map $S_{n+1} = T[S_n]$ whose explicit form is given in Refs. [27,28]. For $S = 1$, $A = 1$, $\tau = 2\pi$, $\lambda = 0.1437002\dots$ the spin map exhibits attractor merging crisis at $B_c = 1.2$: for $B < B_c$ two separate symmetric chaotic attractors, corresponding to the spin “up” ($S_z > 0$) and “down” ($S_z < 0$) orientations, coexist, whereas for $B > B_c$ the attractors merge and the spin jumps between these two orientations. In order to investigate SR $B(n) = B_0 + B_1 \cos(\omega_0 n)$ is assumed, and the TC events are defined as the jumps between the two equivalent spin orientations. The following identification of parameters can be made: $q \equiv B - B_c$, $q_0 \equiv B_0 - B_c$, $q_1 \equiv B_1$.

In Figs. 1 and 2 the results from numerical simulations of the above-mentioned systems are shown. In both cases the curves $p(q)$ exhibit clear oscillations superimposed on the power-law trend (Figs. 1(a) and 2(a)). In the case of the Hénon map the basin of escape is non-fractal, and the almost log-periodic normal oscillations dominate (Fig. 1(a)). In the case of the kicked spin map the basin of escape is fractal, and its structure is incommensurate with that of the chaotic saddle; hence $p(q)$ shows irregular oscillations with a dominant role of roughly log-periodic anomalous oscillations (Fig. 2(a)). In both cases noise-free SMR can be clearly seen, i.e., multiple maxima of the SPA (Figs. 1(b) and 2(b)). The origin of the subsequent maxima and their connection to the general power-law trend (1) and the oscillations of the escape probability were discussed in detail in Refs. [10,11].

3. Theoretical results

3.1. The model of the fractal chaotic saddle and basin of escape

In order to analyze theoretically the numerical results on the escape probability and noise-free SMR let us introduce a geometric model of the fractal chaotic saddle and the basin of escape [18,19]. This model incorporates the important topological properties of the two colliding sets, which we assume to remain identical both below and above the crisis point.

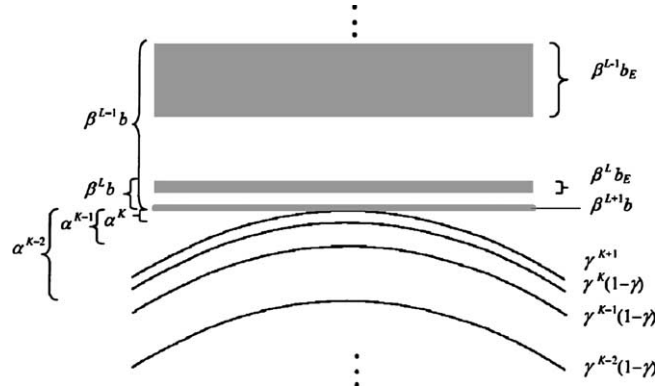


Fig. 3. The model of the fractal chaotic saddle and the fractal basin of escape.

We assume the model of the fractal chaotic saddle \mathcal{A} as a family of $K + 2$ parabolic segments \mathcal{A}_k (Fig. 3)

$$\mathcal{A} = \bigcup_{k=0}^{K+1} \mathcal{A}_k = \bigcup_{k=0}^{K+1} \{(x, y) : y = -x^2 - (1 - \delta_{k,K+1})a\alpha^k + q\}, \tag{2}$$

where a and $\alpha \in (0, 1)$ are model parameters. The invariant measure is uniformly distributed along the segments and its relative density on the segment \mathcal{A}_k is assumed as $\tilde{\mu}_k = (1 - \eta)\eta^k$ for $0 \leq k \leq K$ and $\tilde{\mu}_{K+1} = \eta^{K+1}$, where $0 < \eta < 1$ is another model parameter. The model of the non-fractal basin of escape can be assumed as a half-plane $y > 0$. The model of the fractal basin of escape is in turn assumed as a family of $L + 2$ stripes \mathcal{B}_l (Fig. 3)

$$\mathcal{B} = \bigcup_{l=0}^{L+1} \mathcal{B}_l = \bigcup_{l=0}^{L+1} \{(x, y) : (1 - \delta_{l,L+1})(\beta^l b - \beta^l b_E) \leq y \leq \beta^l b\}, \tag{3}$$

where $\beta \in (0, 1)$, b and b_E are again model parameters. Taking larger K, L means a finer approximation of the self-similar fractal sets. The crisis occurs at $q = q_c = 0$ when the uppermost parabolic segment of the saddle \mathcal{A} touches the lowermost stripe of the basin of escape \mathcal{B} or the half-plane $y > 0$. The model parameters $\alpha, \eta, \beta, b_E, a$ and b are determined by the fractal structure of the saddles and basins of escape of the system under study and can be assessed from the consecutive magnified plots of the collision region between the chaotic saddle and the basin of escape [18,19]. In order to model the case with the time-dependent control parameter, q should be replaced with $q(n)$ in Eq. (2).

3.2. The analytic theory for the escape probability and spectral power amplification

From the model of Section 3.1 the mean probability of the escape event and the SPA vs. the control parameter can be evaluated. Consider the model of chaotic saddle (2) creeping into the model basin of escape (3) for $q > q_c = 0$. The escape probability is proportional to the measure $\mu(q)$ of the overlap of the saddle and the basin of escape [16,17]. The latter measure is a sum of overlap measures $\mu_{kl}(q)$ between the individual parabolic segments \mathcal{A}_k of the chaotic saddle and the stripes \mathcal{B}_l of the basin of escape. Thus we obtain

$$p(q) = \zeta \mu(q) = \zeta \sum_{k=0}^{K+1} \sum_{l=0}^{L+1} \mu_{kl}(q), \tag{4}$$

where ζ is the proportionality constant and

$$\mu_{kl}(q) = \mu_k((1 - \delta_{l,L+1})(\beta^l b - \beta^l b_E), q) - \mu_k(\beta^l b, q), \tag{5}$$

where $\mu_k(c, q)$ denotes the measure of the overlap of the segment \mathcal{A}_k and a half-plane $y > c$. The latter measure for small $q - (1 - \delta_{k,K+1})a\alpha^k - c$ can be approximated as

$$\mu_k(c, q) = \tilde{\mu}_k \sqrt{q - (1 - \delta_{k,K+1})a\alpha^k - c} \Theta(q - a(1 - \delta_{k,K+1})\alpha^k - c), \tag{6}$$

where $\Theta(\cdot)$ denotes the Heaviside function.

The above theory predicts the escape probability $p(q)$ with the power-law trend as in Eq. (1), with $\gamma = \log \eta / \log \alpha + 1/2$, and oscillations superimposed on it. In the case of the non-fractal basin of escape the form of $p(q)$ (Eq. (4)) simplifies significantly (only one sum over k remains) and we get log-periodic normal oscillations with the period $\log \alpha$ [19]. In the case of the fractal basin of escape a complex mixture of oscillations appears. The decreasing (against general trend) anomalous sections can usually be distinguished with their basic period $\log \beta$ [18,19].

Let us now consider the case of time-dependent control parameter. In the adiabatic approximation $\omega_0 \rightarrow 0$ the escape probability is slowly time-dependent, $p(q) \rightarrow p(n) \equiv p(q_0 + q_1 \cos(\omega_0 n))$ [2]. Then the height of the peak $S(\omega_0)$ in the power spectral density of the output signal is equal to the square of the absolute value of the Fourier component P_1 of the escape probability $p(n)$ at the frequency ω_0 [26]. Thus

$$\sigma = \frac{|P_1|^2}{q_1^2} = \frac{|\zeta \sum_{k=0}^{K+1} \sum_{l=0}^{L+1} M_{kl,1}|^2}{q_1^2}, \tag{7}$$

where $M_{kl,1}$ are Fourier components at the frequency ω_0 of the functions $\mu_{kl}(n) \equiv \mu_{kl}(q_0 + q_1 \cos(\omega_0 n))$ in Eq. (4). The components $M_{kl,1}$ can be obtained analytically; the respective expressions can be found in Ref. [10].

3.3. The approximate theory for the escape probability and spectral power amplification based on the concept of fractal self-similarity

Let us discuss both the oscillations of escape probability and the noise-free SMR from a perspective of self-similarity of fractal sets, or discrete-scale invariance [20]. For this purpose let us first consider the case of fractal chaotic saddle and non-fractal basin of escape. Taking $K \rightarrow \infty$ in (2), for small q such that $q < a$ and the approximation (6) is valid, the escape probability given by Eqs. (4)–(6) remains invariant with respect to a discrete scaling transformation $q \rightarrow q\alpha^j$, $j = 0, 1, 2, \dots$ up to a scaling factor

$$\eta^{-1} \alpha^{-\frac{1}{2}} p(\alpha q) = p(q). \tag{8}$$

The origin of the prefactors in the above equation is as follows. For $q < a$ the inspection of Eq. (6) reveals that there is such $k = k_{\min}$ that $\mathcal{A}_{k_{\min}}$ is the parabolic segment of the saddle with the lowest index whose top is within the basin of escape $y > 0$. As q is decreased by the factor α this segment moves out of the basin (i.e., $k_{\min} \rightarrow k_{\min} + 1$), hence the invariant measure density of the saddle within the basin is decreased by the factor η . Simultaneously, the length of each parabolic segment within the basin is decreased by the factor $\alpha^{1/2}$. Combination of these two changes of the escape probability leads to Eq. (8).

The invariance property (8) can now be treated as a functional equation for $p(q)$, putting aside the rather complex form (4) obtained from the models. The general solution of (8) can be assumed as a series expansion

$$p(q) = \sum_{n=-\infty}^{\infty} C_n q^{\tilde{\gamma}_n}. \tag{9}$$

Inserting it back into (8) (and bearing in mind that $\exp(i2\pi n) = 1$) we get a spectrum of complex scaling exponents

$$\tilde{\gamma}_n = \frac{1}{2} + \frac{\log \eta}{\log \alpha} + i \frac{2\pi n}{\log \alpha}, \quad n = 0, \pm 1, \pm 2, \dots \tag{10}$$

Keeping only terms with $n = 0, \pm 1$ in the expansion (9), and assuming $C_1 = C_{-1}^*$ because $p(q)$ is real we obtain [20]

$$p(q) \approx C q^\gamma [1 + B \cos(\Omega \log q + \phi)], \tag{11}$$

where $\gamma = \text{Re} \tilde{\gamma}_n = 1/2 + \log \eta / \log \alpha$ and $\Omega = 2\pi / \log \alpha$. It is an expansion of the general function $p(q)$ obeying Eq. (8) in the Fourier series with respect to $\log q$ up to the first-order terms. Eq. (11) describes a function with a general power-law trend with exponent γ and log-periodic oscillations with period $\log \alpha$ superimposed on it, typically found in description of systems with discrete-scale invariance [20–24]. This function can be treated as a simple, closed-form approximation of the curve $p(q)$ given in Eq. (4). It can be fitted to numerical data treating B , C and ϕ as fitting parameters.

If both the chaotic saddle and the basin of escape are fractal sets and their structures are incommensurate, no one discrete scaling transformation similar to Eq. (8) can be written. However, in many cases the anomalous oscillations turn out to dominate over the normal ones. Then, in the first approximation, the fractal structure of the saddle can be neglected, and only that of the basin of escape taken into account. Neglecting the fractal structure of the chaotic saddle is equivalent to assuming the plain power scaling law (1) for the escape probability, with $\gamma = 1/2 + \log \eta / \log \alpha$. In this approximation the equation corresponding to Eq. (8) becomes $\beta^{-\gamma} p(\beta q) = p(q)$, which yields again the solution of the

form (11) with $\Omega = 2\pi/\log \beta$. The escape probability becomes then log-periodic with period $\log \beta$. However, this approximation of $p(q)$ is usually much worse than in the case of the non-fractal basin of escape. Better analysis of this case would require considering the effect of two competing incommensurate log-periodicities hidden in the system, that of the fractal chaotic saddle and of the fractal basin of escape. Unfortunately, to our knowledge, a general theory of discrete-scale invariance with multiple log-periodicities is not yet known [20]: so far, extension of Eq. (11) to include higher harmonics was only proposed [29]. Thus we constraint ourselves to the above-mentioned approximation.

In the case of time-dependent control parameter $q(n) = q_0 + q_1 \cos(\omega_0 n)$, assuming small q_1 , one can expand $p(n)$ in the Taylor series $p(n) \approx p(q_0) + (dp/dq)_{q_0} q_1 \cos(\omega_0 n)$. The Fourier component P_1 of $p(n)$ at the frequency ω_0 in this approximation is $P_1 = (q_1/2)(dp/dq)_{q_0}$. Assuming $p(q)$ as in Eq. (11) and using the first equation in (7) we obtain for the SPA

$$\sigma = \frac{1}{4} \left| \left(\frac{dp}{dq} \right)_{q_0} \right|^2 = \frac{1}{4} \left| C \gamma q^{\gamma-1} \left\{ 1 + B \sqrt{1 + \left(\frac{\Omega}{\gamma} \right)^2} \cos \left[\Omega \log q + \phi + \arccos \frac{\gamma}{\sqrt{\Omega^2 + \gamma^2}} \right] \right\} \right|^2. \quad (12)$$

From this formula it follows that if $p(q)$ shows log-periodic oscillations around the power-law trend the SPA should possess many maxima which are connected with the subsequent oscillations of the escape probability, and that these maxima should also show log-periodicity with the same period. It should be mentioned that the expansion of $p(n)$ in the Taylor series is possible only for $q_0 \geq q_1$; otherwise for $q_0 + q_1 \cos(\omega_0 n) < 0$ there is $p(n) \equiv 0$, and the function $p(n)$ is not differentiable for all n . It is known [11] that the distinct maxima of the curve SPA vs. q_0 connected with the oscillations of the escape probability appear for $q_0 > q_1$, at $q_0 \approx q_1$ there is a maximum resulting from the main power-law trend of the curve $p(q)$, while for $-q_1 < q_0 < q_1$ there are small, almost invisible maxima or inflexion points located at the rising slope of the latter maximum, connected again with the oscillations of the escape probability. Thus Eq. (12) approximates the SPA in the important region of the control parameter where SMR with distinct maxima can be observed.

4. Comparison with numerical results and discussion

Choosing properly the model parameters and using Eq. (4) one can reproduce the complicated dependence of the escape probability on the control parameter with high accuracy (Figs. 1(a) and 2(a)). The agreement between the numerical and theoretical results is very good in the case of the Hénon map, while in the case of the kicked spin map the overlap of two fractal sets produces a complicated curve $p(q)$ whose fine details cannot be very well captured by a simple model of Section 3.1. Fitting the curves $p(q)$ with Eq. (11) reveals the basic log-periodicity of the escape probability as a function of the control parameter: in the case of the Hénon map it results from the self-similarity of the fractal chaotic saddle, while in the case of the spin map—from the self-similarity of the fractal basin of escape. The curve $p(q)$ for the Hénon map is in fact well approximated by Eq. (11) apart from the region far from the crisis; it is obvious since in this case there is only one fractal set, so the model and Eq. (8) are quite accurate. On the other hand, deviations from the log-periodicity of the escape probability for the kicked spin map are more pronounced.

Choosing the same model parameters as when fitting the escape probability, using Eq. (7) one can also reproduce the complicated multip peaked dependence of the SPA on the control parameter at least qualitatively (Figs. 1(b) and 2(b)). In turn, Eq. (12) yields curves $\sigma(q_0)$ which only roughly resemble the numerical ones (it should be remembered that Eq. (12) is valid only for $q_0 > q_1$). The predicted basic log-periodicity of the sequence of the maxima of the SPA is present, although difficult to observe in numerical curves $\sigma(q_0)$. This is since it can be best seen only close to crisis and for small q_1 , which requires prohibitively long simulation time to obtain the SPA. In the case of the Hénon map an interesting point is that the full analytic theory, Eq. (7), predicts the increase of the height of the maxima of the SPA far from crisis, while the approximate formula (12) predicts their decrease. The latter conclusion seems to be confirmed by the height of the rightmost numerical maximum of the SPA in Fig. 1(b); this is, however, misleading, since far from the crisis the curve $p(q)$ in Fig. 1(a) deviates from both model curves given by Eqs. (4) and (11), hence the height of the above-mentioned maximum cannot be used as a test of validity of the models. In the case of the kicked spin map large deviations from the predictions of Eq. (12) can be seen, and the curve $\sigma(q_0)$ is much more complicated than expected from the simple analysis based on discrete-scale invariance. The presence of the fractal structure of the chaotic saddle, i.e., of the second competing log-periodicity, splits and shifts the maxima of the SPA with respect to what can be supposed if only the basic fractal structure of the basin of escape is taken into account.

5. Summary and conclusions

In this paper two exemplary systems with crises were investigated, exhibiting noise-free SMR resulting from the normal and anomalous oscillations superimposed on the power-law trend of the escape probability from the precritical

attractor as a function of the control parameter. Both the oscillations and the multiple maxima of the SPA appear as a result of collision of the fractal chaotic saddle with the, possibly fractal, basin of escape above the crisis point. Numerical results were compared to theoretical ones, based on a geometric model of the colliding fractal sets. The full analytic theory yields qualitative agreement with numerical results and reproduces irregular oscillations of the escape probability and a complicated structure of the maxima of the SPA. The approximate theory based on the concept of fractal self-similarity, or discrete-scale invariance, captures the basic log-periodicity of the oscillations of the escape probability and of the maxima of the SPA, but fails in reproducing details of these curves. This is particularly visible in the case of fractal basin of escape, in which the SMR results from a collision of two sets with incommensurate fractal structures, and the deviations from log-periodicity are significant.

The results of this paper reveal similarities between systems close to crisis exhibiting noise-free SMR introduced in Refs. [10,11] and a class of systems with external noise exhibiting SMR [13,14]. In both cases the origin of SMR can be associated with the underlying invariance of the important features of the system (the escape probability from the precritical attractor or the potential forces) with respect to a discrete scaling transformation, which leads to basic log-periodicity of the maxima of the SPA. This indicates that log-periodicity can be an universal property of SMR in different kinds of systems. Note, however, that in the chaotic systems near crises the SMR and log-periodicity of maxima appears naturally as a consequence of self-similarity of fractals, and not due to an arbitrarily introduced particular form of a potential. Thus such systems fall naturally into a rich class of systems with discrete-scale invariance [20–24]. On the other hand, chaotic maps close to crisis in the case of fractal basin of escape are exemplary systems with SMR in which the structure of the maxima of the SPA can be more complicated than expected from considerations based on the simplest concept of discrete-scale invariance. Similar complicated structures can be probably also found in stochastic systems more general than the models for SMR considered so far in Refs. [13,14].

Acknowledgements

This work was supported by the Polish Committee for Scientific Research under grant no. 5 P03B 007 21. S.M. acknowledges support by the DAAD scholarship for the stay at the Institute of Physics, Humboldt University at Berlin.

References

- [1] Benzi R, Sutera A, Vulpiani A. The mechanism of stochastic resonance. *J Phys* 1981;14:L453–8.
- [2] McNamara B, Wiesenfeld K. Theory of stochastic resonance. *Phys Rev A* 1989;39:4854–69.
- [3] Jung P, Hänggi P. Amplification of small signals via stochastic resonance. *Phys Rev A* 1991;44:8032–42.
- [4] Gammaitoni L, Hänggi P, Jung P, Marchesoni F. Stochastic resonance. *Rev Mod Phys* 1998;70:223–87.
- [5] Anishchenko VS, Neiman AB, Moss F, Schimansky-Geier L. Stochastic resonance: noise-enhanced order. *Physics—Uspekhi* 1999;42:7–36 (*Usp Fiz Nauk* 1999;169:7–36).
- [6] Anishchenko VS, Neiman AB, Safanova MA. Stochastic resonance in chaotic systems. *J Stat Phys* 1993;70:183–96.
- [7] Crisanti A, Falcioni M, Paladin G, Vulpiani A. Stochastic resonance in deterministic chaotic systems. *J Phys A* 1994;27:L597–603.
- [8] Reibold E, Just W, Becker J, Benner H. Stochastic resonance in chaotic spin-wave dynamics. *Phys Rev Lett* 1997;78:3101–4.
- [9] Chizhevsky VN, Vilaseca R, Corbalán R. Amplification of non-resonant signals via stochastic resonance in a chaotic CO₂ laser. *Phys Rev E* 2000;61:6500–5.
- [10] Matyjaśkiewicz S, Krawiecki A, Hołyst JA, Kacperski K, Ebeling W. Stochastic multiresonance in a chaotic map with fractal basins of attraction. *Phys Rev E* 2001;63:1–10.
- [11] Krawiecki A, Matyjaśkiewicz S, Kacperski K, Hołyst JA. Noise free stochastic multiresonance near chaotic crises. *Phys Rev E* 2001;64:1–4.
- [12] Arai K, Yoshimura K, Mizutani S. Dynamical origin of deterministic stochastic resonance. *Phys Rev E* 2002;65:1–4.
- [13] Vilar JMG, Rubí JM. Stochastic multiresonance. *Phys Rev Lett* 1997;78:2882–5.
- [14] Vilar JMG, Rubí JM. Scaling concepts in periodically modulated noisy systems. *Physica A* 1999;264:1–14.
- [15] Shiao Y-H, Néda Z. A novel resonance in n-GaAs diodes. *Jpn J Appl Phys* 2001;40:6675–6.
- [16] Grebogi C, Ott E, Yorke JA. Critical exponents of chaotic transients in nonlinear dynamical systems. *Phys Rev Lett* 1986;57:1284–7.
- [17] Grebogi C, Ott E, Romeiras F, Yorke JA. Critical exponents for crisis-induced intermittency. *Phys Rev A* 1987;36:5365–80.
- [18] Kacperski K, Hołyst JA. Anomalous oscillations of average transient lifetimes near crises. *Phys Lett A* 1999;254:53–8.
- [19] Kacperski K, Hołyst JA. Theory of oscillations in average crisis-induced transient lifetimes. *Phys Rev E* 1999;60:403–7.
- [20] Sornette D. Discrete-scale invariance and complex dimensions. *Phys Rep* 1998;297:239–70.
- [21] Bernasconi J, Schneider WR. Diffusion in random one-dimensional systems. *J Stat Phys* 1983;30:355–62.
- [22] Saleur H, Sammis CG, Sornette D. Discrete scale invariance, complex fractal dimensions, and log-periodic fluctuations in seismicity. *J Geophys Res* 1996;101:17661–77.

- [23] Sornette D, Johansen A, Bouchaud J-P. Stock market crashes, precursors and replicas. *J Phys I (France)* 1996;6:167–75.
- [24] Vandewalle N, Boveroux Ph, Minguet A, Ausloos M. The crash of October 1987 seen as a phase transition: amplitude and universality. *Physica A* 1998;255:201–10;
Vandewalle N, Ausloos M. How the financial crash of Oct. 27, 1997 could have been predicted. *Eur J Phys B* 1998;4:139–41;
Vandewalle N, Ausloos M, Boveroux Ph, Minguet A. Visualizing the log-periodic pattern before crashes. *Eur J Phys B* 1999;9:355–9.
- [25] Gingl Z, Kiss LB, Moss F. Non-dynamical stochastic resonance: theory and experiments with white and arbitrarily coloured noise. *Europhys Lett* 1995;29:191–5.
- [26] Chapeau-Blondeau F. Stochastic resonance in the Heaviside nonlinearity with white noise and arbitrary periodic signal. *Phys Rev E* 1995;53:5469–72.
- [27] Hołyst JA, Sukiennicki A. Regular and chaotic behavior of a kicked damped spin. *Acta Phys Polonica A* 1992;81:353–60.
- [28] Hołyst JA, Sukiennicki A. Chaotic dynamics of a damped classical spin. *J Magn Magn Mater* 1992;104–107:2111–2.
- [29] Johansen A, Sornette D. Financial “anti-bubbles”: log-periodicity in gold and Nikkei collapses. *Int J Mod Phys C* 1999;10:563–75.